Cellular/Molecular

Presynaptic Control of Striatal Glutamatergic Neurotransmission by Adenosine A_1–A_{2A} Receptor Heteromers

Francisco Ciruela,[1] Vicent Casadó,[1] Ricardo J. Rodrigues,[2] Rafael Luján,[3] Javier Burgueño,[4] Meritxell Canals,[1] Janusz Borycz,[5] Nelson Rebola,[2] Steven R. Goldberg,[5] Josefa Mallol,[1] Antonio Cortés,[1] Enric I. Canela,[1] Juan F. López-Giménez,[6] Graeme Milligan,[6] Carme Lluis,[1] Rodrigo A. Cunha,[2] Sergi Ferré,[5] and Rafael Franco[1]

[1]Department of Biochemistry and Molecular Biology, University of Barcelona, 08028 Barcelona, Spain, [2]Centre for Neuroscience of Coimbra, Institute of Biochemistry, Faculty of Medicine, University of Coimbra, 3004-504 Coimbra, Portugal, [3]Facultad de Medicina and Centro Regional de Investigaciones Biomédicas, Universidad de Castilla-La Mancha, 02006 Albacete, Spain, [4]Target Validation, Laboratoris Dr. Esteve, Parc Científic de Barcelona, 08028 Barcelona, Spain, [5]Behavioral Neuroscience Branch, National Institute on Drug Abuse, Intramural Research Program, National Institutes of Health, Department of Health and Human Services, Baltimore, Maryland 21224, and [6]Division of Biochemistry and Molecular Biology, Institute of Biomedical and Life Sciences, University of Glasgow, Glasgow G12 8QQ, United Kingdom

The functional role of heteromers of G-protein-coupled receptors is a matter of debate. In the present study, we demonstrate that heteromerization of adenosine A_1 receptors (A_1Rs) and A_{2A} receptors (A_{2A}Rs) allows adenosine to exert a fine-tuning modulation of glutamatergic neurotransmission. By means of coimmunoprecipitation, bioluminescence and time-resolved fluorescence resonance energy transfer techniques, we showed the existence of A_1R–A_{2A}R heteromers in the cell surface of cotransfected cells. Immunogold detection and coimmunoprecipitation experiments indicated that A_1R and A_{2A}R are colocalized in the same striatal glutamatergic nerve terminals. Radioligand-binding experiments in cotransfected cells and rat striatum showed that a main biochemical characteristic of the A_1R–A_{2A}R heteromer is the ability of A_{2A}R activation to reduce the affinity of the A_1R for agonists. This provides a switch mechanism by which low and high concentrations of adenosine inhibit and stimulate, respectively, glutamate release. Furthermore, it is also shown that A_1R–A_{2A}R heteromers constitute a unique target for caffeine and that chronic caffeine treatment leads to modifications in the function of the A_1R–A_{2A}R heteromer that could underlie the strong tolerance to the psychomotor effects of caffeine.

Key words: **adenosine A_1 receptor; adenosine A_{2A} receptor; heteromeric receptors; glutamate; striatum; caffeine**

Introduction

Of the four known adenosine receptors (A_1, A_{2A}, A_{2B}, and A_3), A_1 receptor (A_1R) and A_{2A} receptor (A_{2A}R) are primarily responsible for the central effects of adenosine (Dunwiddie and Masino, 2001). The same receptors are also the main target of nontoxic psychostimulant doses of caffeine, the most consumed psychoactive drug in the world (Fredholm et al., 1999). In addition to their postsynaptic location in different brain regions, A_1R and A_{2A}R can be found presynaptically. A_1R and A_{2A}R are coupled to $G_{i/o}$- and $G_{s/olf}$-proteins, respectively (Dunwiddie and Masino, 2001). Stimulation of presynaptic A_1Rs receptors decreases the probability of neurotransmitter release, whereas activation of presynaptic A_{2A}Rs enhances neurotransmitter release (Yawo and Chuhma, 1993; Wu and Saggau, 1997; O'Kane and Stone, 1998; Lopes et al., 2002; Quarta et al., 2004b).

Previous studies have provided evidence for functional antagonistic interactions between A_1Rs and A_{2A}Rs that modulate glutamate release in the striatum and hippocampus (O'Kane and Stone, 1998; Lopes et al., 2002; Quarta et al., 2004b). The coexistence of both facilitatory A_{2A}Rs and inhibitory A_1Rs in the same terminal is intriguing, particularly in view of their opposite functional effects. In the present study, we use radioligand-binding, coimmunoprecipitation, bioluminescence resonance energy transfer (BRET) and time-resolved fluorescence resonance energy transfer (TR-FRET) techniques to demonstrate that A_1R and A_{2A}R form A_1R–A_{2A}R heteromers in mammalian cells and in striatal glutamatergic nerve terminals. The main biochemical characteristic of the A_1R–A_{2A}R heteromer is the ability of A_{2A}R activation to reduce the affinity of the A_1R for agonists, providing a switch mechanism by which low and high concentrations of adenosine inhibit and stimulate, respectively, glutamatergic neurotransmission. The present study is the first indication that heteromerization of different receptors for the same modulator constitutes a unique way to presynaptically regulate neurotransmission and also is the first indication that A_1R–A_{2A}R heteromers may be involved in the acute and chronic effects of caffeine.

Received Aug. 23, 2005; revised Jan. 9, 2006; accepted Jan. 10, 2006.

This work was supported by Ministerio de Ciencia y Tecnología Grant SAF2002-03293 (R.F.), Fundació La Marató de TV3 Grant Marató/2001/012710 (R.F.), Fundacio la Caixa Grant 02/056-00 (R.F.), and Fundação para a Ciência e para a Tecnologia Grant POCTI/SAU-FCF/59601/2004 (R.A.C.), as well as by National Institute on Drug Abuse intramural research funds. F.C. is currently holding a Ramón y Cajal research contract signed with the Ministerio de Ciencia y Tecnología.

Correspondence should be addressed to Sergi Ferré, National Institute on Drug Abuse, Intramural Research Program, National Institutes of Health, Department of Health and Human Services, 5500 Nathan Shock Drive, Baltimore, MD 21224. E-mail: sferre@intra.nida.nih.gov.

DOI:10.1523/JNEUROSCI.3574-05.2006

 0270-6474/06/262080-08$15.00/0

Materials and Methods

Animals, cell culture, and transfection. Male Sprague Dawley or Wistar rats (Charles River Laboratories, Wilmington, MA) were used, where indicated. Caffeine was administered chronically by giving free access to bottles containing a solution of 1.0 mg/ml caffeine anhydrate base (Sigma, St. Louis, MO) in tap water for 14 d (chronic group) as the only fluid available for drinking. HEK-293 cells were grown in DMEM (Sigma) as described previously (Ciruela et al., 2001; Canals et al., 2003). All animal experiments were performed in accordance with the National Institutes of Health and *Guidelines for the Care and Use of Mammals in Neuroscience and Behavioral Research* (National Research Council, 2003). Cells were transiently transfected with the DNA encoding for the proteins specified in each case by calcium phosphate precipitation. The human hemagglutinin (HA)-A_{2A}R and Flag-A_1R construct were obtained as previously described (Ciruela et al., 2001; Canals et al., 2003). These receptors were also subcloned in frame with either *Renilla* luciferase (A_{2A}R-*R*luc) or with the enhanced yellow fluorescent protein (A_1R-YFP).

Immunoprecipitation and Western blot analysis. Transiently transfected HEK cells or striatal synaptosomes were solubilized in ice-cold lysis buffer [PBS, pH 7.4, containing 1% (v/v) Nonidet P-40] for 30 min on ice. The solubilized preparation was then centrifuged at 13,000 × *g* for 30 min, and the supernatant (1 mg/ml) was processed for immunoprecipitation, as described previously (Ciruela et al., 2001; Canals et al., 2003). Immune complexes in sample buffer (8 M urea, 2% SDS, 100 mM DTT, 375 mM Tris, pH 6.8) were dissociated by heating to 37°C for 2 h and resolved by SDS-PAGE. Proteins were transferred to polyvinylidene difluoride membranes using a semidry transfer system and immunoblotted with the indicated primary antibody. The blots were then incubated with a secondary horseradish peroxidase (HRP)-conjugated goat anti-rabbit IgG antibody (1:60,000). The immunoreactive bands were developed using a chemiluminescent detection kit. The primary antibodies used were as follows: anti-Flag monoclonal antibody and anti-HA monoclonal antibody (Sigma) and rabbit anti-A_{2A}R and anti-A_1R polyclonal antibodies (Affinity BioReagents, Golden, CO). To test the specificity of the anti-A_1R polyclonal antibody in striatal tissue, a preincubation with the immunizing peptide C(309)QPKPPIDEDLPEEKAED(326) (ab5893; Abcam, Cambridge, MA) was performed. This preincubation completely abrogated the staining observed in striatal tissue (data not shown).

Immunostaining. For immunochemistry, transiently transfected HEK cells or rat striatal synaptosomes were fixed in 4% paraformaldehyde for 15 min and washed with PBS containing 20 mM glycine (buffer A) to quench the aldehyde groups. Then, after permeabilization with buffer A containing 0.2% Triton X-100 for 5 min, cells or striatal synaptosomes were treated with PBS containing 1% bovine serum albumin (buffer B). After 1 h at room temperature, cells or synaptosomes were labeled with the indicated primary antibody for 1 h, washed, and stained with the indicated secondary antibody. Samples were rinsed and observed in a confocal microscope (Ciruela et al., 2001; Canals et al., 2003; Rodrigues et al., 2005). The primary antibodies used were as follows: anti-HA monoclonal antibody (2 μg/ml; Sigma), rabbit anti-Flag polyclonal antibody (2 μg/ml; Sigma), mouse anti-A_{2A}R (2 μg/ml; Upstate Biotechnology, Lake Placid, NY), rabbit anti-A_1 receptor (1:200; Affinity Bioreagents), guinea pig anti-vGluT1 (1:5000; Chemicon, Temecula, CA) and guinea pig anti-vGluT2 (1:5000; Chemicon). The secondary antibodies used were as follows: Alexa Fluor 488-conjugated goat anti-mouse IgG (1:200; Invitrogen, Eugene, OR), Texas Red-conjugated goat anti-rabbit IgG (1:1000; Invitrogen), Alexa Fluor 598-conjugated goat anti-guinea pig (1:200; Invitrogen), and Alexa Fluor 350-conjugated goat anti-rabbit (1:200; Invitrogen). For ultrastructural analysis, preembedding techniques for single and double labeling were used, as described previously (Lujan et al., 1996). Briefly, free-floating sections were incubated in Tris-buffered saline containing 10% of normal goat serum (TBS-NGS) during 1 h. After blocking, sections were incubated during 48 h with TBS-NGS containing mouse anti-A_{2A}R antibody (2 μg/ml; Upstate Biotechnology) and/or rabbit-anti-A_1R antibody (2 μg/ml; Affinity Bioreagents). When a single primary antibody was used, it was visualized by the silver-intensified immunogold reaction. When two primary antibodies were used, one of them (anti-A_{2A}R antibody) was visualized by the immunoperoxidase reaction and the second one (anti-A_1R antibody) by the silver-intensified immunogold reaction. The following secondary antibodies were used: goat anti-rabbit coupled to 1.4 nm gold, goat anti-mouse coupled to 1.4 nm gold, and biotinylated goat anti-mouse antibody. After washing in TBS, sections were processed and observed as described previously (Lujan et al., 1996).

BRET and TR-FRET. Forty-eight hours after transfection, HEK cells were rapidly washed twice in PBS, detached, and resuspended in the same buffer. The protein was determined using a Bradford assay kit (Bio-Rad, Hercules, CA). To quantify A_{2A}R-*R*luc and A_1R-YFP expression, a cell suspension (20 μg of protein) was distributed in duplicate into 96-well transparent bottom microplates (Corning, Corning, NY). The fluorescence and luminescence were determined as described previously (Canals et al., 2003). For BRET measurement, 20 μg of cell suspension was distributed in duplicate in 96-well opaque microplates (Corning) and 5 mM coelenterazine H was added. After 1 min, the readings were collected by using a Fusion microplate analyzer (Packard, Meridian, CT) that allows the integration of the signals using filters with the appropriate bandpass. The BRET ratio is defined as [(emission at 510–590)/(emission 440–500)] − cf., where cf. corresponds to (emission at 510–590)/(emission at 440–500) for the A_{2A}R-*R*luc construct expressed alone in the same experiment. Time-resolved FRET was performed as described previously (McVey et al., 2001). Briefly, transiently transfected HEK cells were detached, washed twice with PBS, and incubated in PBS containing 50% fetal bovine serum and 5 nM Eu^{3+}-labeled anti-Flag antibody (CIS bio, Gif/Yvette, France) and 20 nM allophycocyanin-labeled anti-HA antibody (CIS bio) during 3 h in constant rotation at room temperature. After washing, cells were placed into a 96-well microtiter plate and analyzed using a Victor^2 (PerkinElmer, Wellesley, MA) configured for time-resolved fluorescence.

Radioligand-binding experiments. Membrane suspensions from rat striatum or from transfected HEK cells were obtained as described previously (Casadó et al., 1990; Herrera et al., 2001). Displacement experiments were performed by incubating (120 min) membranes (0.25 mg/ml striatal protein or 0.19 mg/ml HEK cells) at 25°C in 50 mM Tris-HCl buffer, pH 7.4, containing 10 mM $MgCl_2$ and 2 U/ml adenosine deaminase (EC 3.5.4.4; Roche, Basel, Switzerland) with the indicated concentrations of ^{3}H-labeled *R*-phenylisopropyladenosine ([^{3}H]R-PIA) (30.5 Ci/mmol; Moravek Biochemicals, Brea, CA) or ^{3}H-labeled 2-*p*-(2-carboxyethyl)phenethylamino-5′-*N*-ethylcarboxamido adenosine HCl ([^{3}H]CGS21680) (45 Ci/mmol; PerkinElmer) in the absence or presence of increasing concentrations of nonlabeled compounds (Sarrió et al., 2000). Nonspecific binding was determined in the presence of 10 μM 1,3-dipropyl-8-cyclopentylxanthine (DPCPX) (Sigma) for A_1Rs or 10 μM ZM241385 (4-(2-[7-amino-2-(2-furyl)[1,2,4]triazolo[2,3-a][1,3,5]triazin-5-ylamino]ethyl)phenol) (Tocris, Ellisville, MO) for binding to A_{2A}Rs. Free and membrane-bound ligand were separated and detected as described previously (Casadó et al., 1990; Sarrió et al., 2000; Herrera et al., 2001). Radioligand displacement curves were analyzed by nonlinear regression using commercial program GRAFIT (Erithacus Software, Surrey, UK) by fitting the total binding data to the displacement models with one- or two-affinity sites (Cheng and Prusoff, 1973; Casadó et al., 1992). Values are parameter ± SEM and differences with respect to controls were tested for significance ($p < 0.05$) using Student's *t* test for unpaired samples. Goodness of fit was tested according to reduced χ^2 value given by the nonlinear regression program GRAFIT. A modified *F* test was used to analyze whether the fit to the two-site model significantly improved on the fit to one-site model, and $p < 0.05$ was taken as a criterion of significance; when no significant improvement over the one-site model was detected, the *p* values were >0.30.

Calcium determination. Transiently transfected HEK cells (10^6 cells/ml) were loaded with 5 mM fura-2 AM for 30 min at 37°C. After washing the cells, calcium peak induction was achieved by the addition of 50 nM R-PIA and/or 200 nM CGS21680. Intracellular calcium was determined as described previously (Ciruela et al., 2001).

Striatal synaptosomes preparation and measurement of evoked [^{3}H]glutamate release. Striatal synaptosomes prepared for immunocytochemical analysis were obtained through a discontinuous Percoll gradient (Ro-

drigues et al., 2005). The release of [^{3}H]glutamate from rat striatal nerve terminals was performed as described previously (Lopes et al., 2002; Rodrigues et al., 2005). The synaptosomes were stimulated with 20 mM K^+ (isomolar substitution of NaCl by KCl in the Krebs' solution) at 3 and 9 min after starting sample collection (S_1 and S_2). Tested drugs were added 2 min before S_2 onward, whereas modifiers present in S1 and S2 were added from 10 min before starting sample collection onward. Radioactivity was expressed in terms of disintegrations per second per milligram of protein (becquerels per milligram) in each chamber. The percentage of modification of the evoked release caused by the tested drugs was determined by measuring the percentage of modification of the ratio S2/S1 in comparison with the ratio S2/S1 of the respective control. Adenosine (0.1–100 μM), N^6-cyclopentyladenosine (CPA) (100 nM), CGS (10 nM), DPCPX (50 nM), and 5-amino-7-(2-phenylethyl)-2-(2-furyl)-pyrazolo[4,3-e]-1,2,4-triazolo[1,5-c]pyrimidine (SCH58261) (50 nM), when present during S1 and S2, did not cause any effect per se on the S2/S1 ratio. We further confirmed that the presence of either CPA or CGS21680 during S1 and S2 did not lead to a desensitization of the A_1R-mediated or A_{2A}R-mediated modulation of glutamate release; in fact, when applied during S1 and S2, CGS21680 (10 nM) enhanced glutamate release by 28.5 ± 1.8% during S1 and by 34.9 ± 3.6% during S2, whereas CPA (100 nM) inhibited glutamate release by 10.8 ± 0.7% during S1 and by 10.4 ± 1.0% during S2 ($n = 6$).

Results

A_1R–A_{2A}R heteromers in the cell surface of transfected cells

From extracts of HEK cells transiently transfected with Flag-A_1Rs and HA-A_{2A}Rs, the mouse anti-Flag antibody coimmunoprecipitated a band of ~42 kDa, which corresponds to the HA-A_{2A}R (Fig. 1*a*). This band did not appear in immunoprecipitates from cells only transfected with the cDNA for either HA-A_{2A}Rs or Flag-A_1Rs (Fig. 1*a*). Conversely, in extracts from these cells, the anti-HA antibody coimmunoprecipitated a band of ~38 kDa corresponding to the Flag-A_1R (Fig. 1*a*).

A_1R–A_{2A}R heteromerization was tested using BRET assays. A positive and saturable BRET signal for the transfer of energy between A_{2A}R-*R*luc and A_1R-YFP was obtained (Fig. 1*b*) in cells cotransfected with a constant concentration of the A_{2A}R-*R*luc and increasing concentrations of A_1R-YFP. As the pair A_{2A}R-*R*luc and GABA receptor $GABA_{B2}$-YFP led to an undetectable BRET signal (Fig. 1*b*), the hyperbolic BRET signal found for the A_{2A}R-*R*luc plus A_1R-YFP argues for the selectivity of the interaction between A_1Rs and A_{2A}Rs, and also suggest that the distance between donor (A_{2A}R-*R*luc) and acceptor (A_1R-YFP) is ≤10 nm. To assess whether these A_1R–A_{2A}R heteromers occur at the plasma membrane level, TR-FRET was assayed in cells cotransfected with Flag-A_1Rs and HA-A_{2A}Rs. Because Flag and HA tags were localized extracellularly at the N terminus of these receptors, only the A_1Rs and A_{2A}Rs localized at the plasma membrane of intact cells were detected and gave a positive strong TR-FRET signal (acceptor/donor emission, mean ± SEM, 0.081 ± 0.002; $n = 3$) compared with a mixture of cells previously transfected with only A_1Rs or A_{2A}Rs and then mixed before the assays (acceptor/donor emission, 0.011 ± 0.002; $n = 3$). Confocal microscopy analysis of nonpermeabilized HEK cells transfected with the cDNAs for Flag-A_1Rs and HA-A_{2A}Rs confirmed an overlapped distribution of the two proteins on the cell surface (Fig. 1*c*).

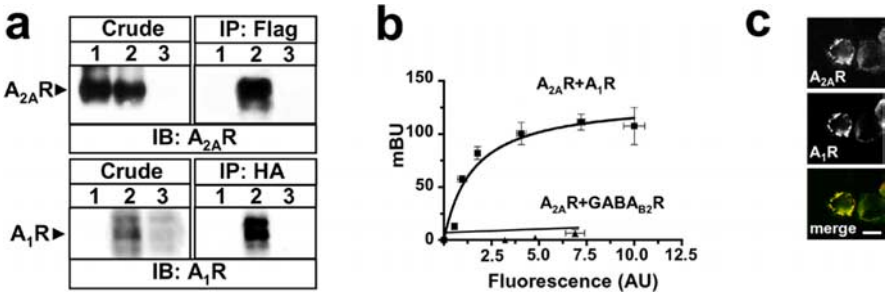

Figure 1. A_1R–A_{2A}R heteromerization in HEK cells. ***a***, Coimmunoprecipitation of A_1Rs and A_{2A}Rs. HEK-293 cells transiently expressing HA-A_{2A}Rs alone (lane 1), HA-A_{2A}Rs plus Flag-A_1Rs (lane 2), or Flag-A_1Rs (lane 3) were washed, solubilized, and processed for immunoprecipitation using anti-Flag monoclonal antibody (2 μg/ml; IP:Flag) or anti-HA monoclonal antibody (2 μg/ml; IP:HA). Solubilized membranes (Crude) and immunoprecipitates (IP) were analyzed by SDS-PAGE and immunoblotted using rabbit anti-A_{2A}R polyclonal antibody (1:2000) or rabbit anti-A_1R polyclonal antibody (1:1000) and HRP-conjugated goat anti-rabbit IgG as a secondary antibody. These blots are representative of four different experiments with similar qualitative results. IB, Immunoblot. ***b***, BRET saturation curve. BRET was measured in HEK-293 cells coexpressing A_{2A}R-*R*luc and A_1R-YFP (■) or A_{2A}R-*R*luc and $GABA_B$R2-YFP (▲) constructs. Cotransfections were performed with increasing amounts of plasmid DNA for the A_1R-YFP construct, whereas the DNA for the A_{2A}R-*R*luc construct was maintained constant. Both fluorescence and luminescence of each sample were measured before every experiment to confirm equal expression of A_{2A}R-*R*luc while monitoring the increase of YFP expression. The saturation curve include results obtained from five independent experiments; mBU is the BRET ratio × 1000 (see Materials and Methods); error bars indicate SD of mean specific BRET ratio (mBU) values of five individual experiments grouped as a function of the amount of fluorescence of the acceptor. AU, Arbitrary unit. ***c***, Cell surface colocalization of A_1Rs and A_{2A}Rs in HEK cells. HEK cells were transfected with A_{2A}R-HA, A_1R-Flag, or both receptors simultaneously (coexpression). Nonpermeabilized cotransfected cells were immunostained with mouse anti-HA monoclonal antibody and rabbit anti-Flag polyclonal antibody. The bound primary antibodies were detected using either Alexa Fluor 488-conjugated goat anti-mouse IgG antibody or Texas Red-conjugated goat anti-rabbit. Cells were analyzed by double immunofluorescence with confocal microscopy. Superimposition of images reveals A_1R–A_{2A}R cell surface colocalization in yellow (merge). Scale bar, 10 μm.

Table 1. Equilibrium dissociation constants of A_1Rs and A_{2A}Rs expressed in HEK cells

Transfection	Radioligand	Displacer	K_D
A_1R	[^{3}H]R-PIA	R-PIA	1.9 ± 0.4 nM
		Caffeine	90 ± 20 μM
A_{2A}R	[^{3}H]CGS21680	CGS21680	110 ± 30 nM
		Caffeine	7 ± 1 μM
A_1R + A_{2A}R	[^{3}H]R-PIA	R-PIA	1.9 ± 0.3 nM
		Caffeine	93 ± 33 μM
	[^{3}H]CGS21680	CGS21680	120 ± 40 nM
		Caffeine	90 ± 20 μM*
A_{2A}R + D_2R	[^{3}H]CGS21680	CGS21680	110 ± 40 nM
		Caffeine	5 ± 2 μM

HEK cells were transfected with the indicated receptor. Membranes of these cells were incubated with [^{3}H]R-PIA (0.8 nM) or [^{3}H]CGS21680 (18 nM) in the absence or presence of increasing concentrations of displacer in 50 mM Tris-HCl containing 10 mM $MgCl_2$ and 2 U/ml adenosine deaminase. Data represent means ± SEM. * $p < 0.001$ with respect to both the K_D value for A_{2A}R in single-transfected cells and the K_D value for A_{2A}R plus D_2R-cotransfected cells.

Biochemical characteristics of the A_1R–A_{2A}R heteromers

Radioligand-binding experiments using the A_1R agonist [^{3}H]R-PIA and the A_{2A}R agonist [^{3}H]CGS21680 were performed in A_1R–A_{2A}R cotransfected cells and cells transfected with either A_1Rs or A_{2A}Rs (Table 1). K_D values for the binding of R-PIA to A_1R and for the binding of CGS21680 to A_{2A}R were similar in single- or double-transfected cells (Table 1), indicating that heteromerization does not modify the affinity of the A_1Rs or A_{2A}Rs for agonists. A_1R showed the same K_D for caffeine in A_1R as in A_1R–A_{2A}R transfected cells (Table 1). In single-transfected cells,

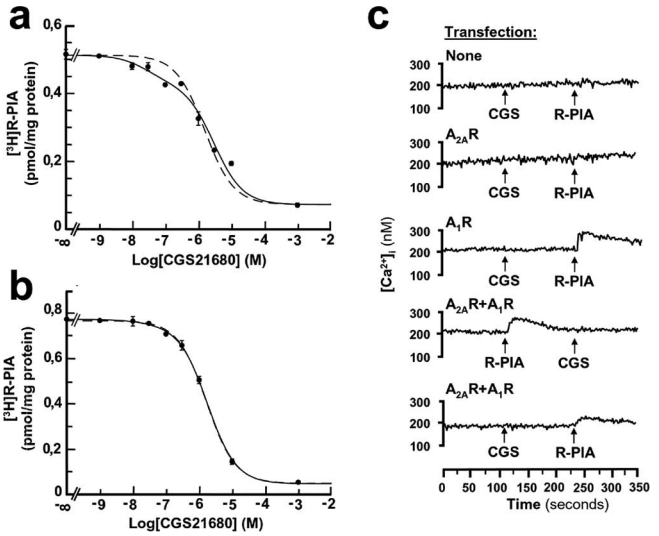

Figure 2. A_{2A}R-mediated modulation of A_1R function in HEK cells. ***a***, ***b***, Modulation of [^{3}H]R-PIA binding to A_1R by A_{2A}R activation. HEK cells were transiently cotransfected with A_1R and A_{2A}R (***a***) or with A_1R alone (***b***). Membranes (0.19 mg/ml) of these cells were incubated with 0.8 nM A_1R agonist [^{3}H]R-PIA in the absence or presence of increasing concentrations of the A_{2A}R agonist CGS21680 in 50 mM Tris-HCl containing 10 mM $MgCl_2$ and 2 U/ml adenosine deaminase. Binding experiments were performed as described in Materials and Methods. The data were adjusted to one single binding site (dashed line) or to two binding sites (solid line). ***c***, Modulation by A_{2A}Rs of A_1R-induced Ca^{2+} mobilization. Transiently transfected HEK-293 cells were loaded with fura-2 AM, and the intracellular Ca^{2+} mobilization was determined after stimulation with R-PIA (50 nM) or CGS21680 (50 nM). The presence of CGS21680 decreases R-PIA-induced Ca^{2+} mobilization in the doubly transfected cells. These recordings are representative of 10 different experiments with similar qualitative results.

A_{2A}Rs displayed higher affinity for caffeine than A_1Rs (Table 1). Interestingly, the affinity of A_{2A}Rs for caffeine in A_1R–A_{2A}R-cotransfected cells was 12-fold lower to that compared with A_{2A}R-transfected cells ($p < 0.001$) (Table 1). The affinity of the A_{2A}R for CGS21680 and caffeine was not altered when cotransfected with the dopamine D_2 receptor (D_2R), although they form A_{2A}R–D_2R heterodimers (Canals et al., 2003) (Table 1).

In cells cotransfected with both A_1Rs and A_{2A}Rs, but not in cells expressing only A_1Rs, the affinity of A_1Rs for [^{3}H]R-PIA decreased in the presence of the A_{2A}R agonist CGS21680, indicating that A_{2A}R activation reduces the affinity of A_1R for its agonist. As illustrated in Figure 2*a*, the displacement of [^{3}H]R-PIA by CGS21680 in membranes from A_1R–A_{2A}R-cotransfected cells was significantly ($p < 0.01$) better fitted by a two-site model than by a single-site model (Fig. 2*a*, solid vs dashed line), whereas it was better fitted ($p < 0.01$) to a single-site model rather than a two-site model in membranes from A_1R single-transfected cells (Fig. 2*b*, solid vs dashed line). At low concentrations of CGS21680, when it binds preferentially to A_{2A}Rs (at concentrations of CGS21680 <500 nM, the direct binding of CGS21680 to A_1Rs is <1%, according to the calculated affinity of A_1R for CGS21680), CGS21680 significantly ($p < 0.05$) decreased the binding of [^{3}H]R-PIA to the A_1R from an EC_{50} value of 3.0 ± 0.4 μM to 30 ± 10 nM (means ± SEM). The EC_{50} value corresponds to one-half of the maximum inhibitory effect of CGS21680 on the binding of [^{3}H]R-PIA to the A_1R (or the high-affinity site calculated using the two-site model). In contrast, the displacement of [^{3}H]CGS21680 by R-PIA was not affected in the membranes from cells cotransfected with A_1Rs and A_{2A}Rs (data not shown). This means that the binding characteristics of A_{2A}Rs are preserved in the A_1R–A_{2A}R heterodimer, whereas the binding characteristics of A_1Rs become controlled by A_{2A}Rs in this heterodimer.

The ability of A_{2A}Rs to decrease A_1R-mediated effects after formation of the A_1R–A_{2A}R heterodimer was confirmed in experiments measuring intracellular calcium levels in HEK cells transiently expressing Flag-A_1Rs plus HA-A_{2A}Rs. The intracellular calcium peak induced by the A_1R agonist, R-PIA (50 nM), was similar in HEK cells transfected with A_1R alone or A_1R plus A_{2A}R (Fig. 2*c*) (95 ± 15 and 86 ± 12 nM, respectively). However, preincubation with 50 nM CGS21680, which was by itself ineffective, significantly reduced the calcium peak obtained in response to A_1R activation in cells doubly transfected with both receptors (Fig. 2*c*) to 41 ± 16 nM. This contrasted with the inability of CGS21680 (50 nM) to affect A_1R-mediated recruitment of intracellular calcium in cells expressing only Flag-A_1Rs. R-PIA (50 nM) or CGS21680 (50 nM) failed to modify intracellular calcium levels in nontransfected HEK-293 cells (Fig. 2*c*).

A_1R–A_{2A}R heteromers in rat striatum

Immunoelectron microscopy, using preembedding immunogold techniques, revealed the presence of A_{2A}R immunoreactivity along the extrasynaptic plasma membrane of axon terminals establishing asymmetric synapses (Fig. 3*a*), as well as in the presynaptic active zone of asymmetric synapses facing dendritic shafts and spines (Fig. 3*b*). A_{2A}Rs were also observed in postsynaptic structures along the extrasynaptic and perisynaptic plasma membrane of dendritic shafts and spines, establishing asymmetrical synapses with axon terminals (Fig. 3*a–c*). Similarly, immunoreactivity for the A_1R was localized along the extrasynaptic plasma membrane and presynaptic active zone of axon terminals in asymmetric synapses and along the extrasynaptic plasma membrane of dendritic shafts and spines (Fig. 3*d*,*e*) establishing asymmetrical synapses with axon terminals. Interestingly, both receptors colocalized in both presynaptic and postsynaptic structures of asymmetrical, putative glutamatergic, synapses (Fig. 3*f–h*). This is the first direct anatomic evidence for adenosine A_{2A}Rs and A_1Rs colocalization in the same neuronal compartments.

To test the presence of A_1R–A_{2A}R heteromers in the rat striatum, competitive-inhibition experiments by CGS21680 of [^{3}H]R-PIA binding were also performed in membrane preparations from rat striatum. As observed in cells cotransfected with A_1Rs and A_{2A}Rs, the obtained displacement data in rat striatal membranes were significantly ($p < 0.001$) better fitted by a two-site model than by a single-site model (Fig. 4*a*). The IC_{50} value, which reflects the binding of CGS21680 directly to the A_1R (low-affinity site calculated using the two-site model), and the EC_{50} value, which refers to the effect of CGS21680 on the binding of R-PIA to A_1R (high-affinity site calculated using the two-site model) were 1.8 ± 0.5 μM and 22 ± 6 nM, respectively (means ± SEM). These values were strikingly similar to those obtained using A_1R–A_{2A}R-cotransfected cells (3.0 ± 0.4 μM and 30 ± 10 nM, respectively). The activation of A_1R with R-PIA did not modify the affinity of A_{2A}R for its agonist CGS21680 in rat striatal membranes (data not shown), as observed in cells cotransfected with A_1Rs and A_{2A}Rs. Another correlate of the existence of A_1R–A_{2A}R heteromers in the striatum, based on the findings obtained in cells cotransfected with A_1Rs and A_{2A}Rs, was that the affinity of rat striatal A_{2A}Rs for caffeine was four times lower than the affinity of A_1Rs for caffeine (see below).

A_1R–A_{2A}R heteromeric complexes in striatal glutamatergic nerve terminals

The preferential colocalization of A_1R and A_{2A}R in glutamatergic terminals was confirmed by immunocytochemistry and coimmunoprecipitation. A_1R and A_{2A}R immunoreactivity could be

detected in single glutamatergic nerve terminals, identified by immunostaining using antibodies against vesicular glutamate transporters type 1 and 2 (vGluT1 and vGluT2), which are expressed in glutamatergic neurons (Fremeau et al., 2001; Herzog et al., 2001) (Fig. 5*a*). Quantification of images ($n = 4$) showed that there is a 61 ± 2% (in means ± SEM) of glutamatergic terminals that are immunoreactive for both A_1Rs and A_{2A}Rs, whereas only 1.5 ± 0.9% are endowed with A_{2A}Rs but not with A_1Rs and 9 ± 1% with A_1Rs but not with A_{2A}Rs (Fig. 5*b*). The number of glutamatergic terminals that do not express any of the receptors is <30%. As shown in Figure 5*c*, an antibody against A_{2A}Rs was able to immunoprecipitate A_1Rs from solubilized rat striatal nerve terminals. These results demonstrate that A_1Rs and A_{2A}Rs can form heteromeric receptor complexes in the striatal nerve terminals.

To prove a direct effect of presynaptic A_1R and A_{2A}R on glutamate release, the evoked release of glutamate was analyzed from superfused rat striatal nerve terminals loaded with [^{3}H]glutamate. The A_1R agonist CPA (100 nM) inhibited (mean ± SEM; 31.6 ± 2.6%, $n = 3$) the K^+-evoked [^{3}H]glutamate release and this effect was prevented by preincubation with the selective A_1R antagonist DPCPX (50 nM) (Fig. 6*a*), which did not have any significant effect on its own (data not shown). The inhibitory effect of CPA was also prevented when synaptosomes were preincubated with the A_{2A}R agonist CGS21680 (10 nM) (Fig. 6*a*), showing the A_{2A}R-mediated negative modulation of A_1R function, as occurred in HEK cells. In contrast, CGS21680 facilitated (57.7 ± 6.4%; $n = 3$) the K^+-evoked [^{3}H]glutamate release, and this effect was prevented by the selective A_{2A} receptor antagonist SCH58261 (50 nM) but was not modified when synaptosomes were preincubated with CPA (Fig. 6*a*). SCH58261 alone did not have any effect on glutamate release (data not shown). When CGS21680 (10 nM) and CPA (100 nM) were simultaneously added, a facilitatory effect was obtained (44.5 ± 8.6%; $n = 6$), which was significantly ($p < 0.05$) higher than the arithmetic sum of the separate effects of 10 nM CGS21680 and 100 nM CPA (i.e., if these effects were purely additive), as illustrated by the dashed bar in Figure 6*a*. Overall, these results agree with the occurrence of functional A_1R–A_{2A}R heteromers in striatal glutamatergic nerve terminals testified by the ability of A_{2A}Rs to abrogate A_1R-mediated effects.

Finally, the addition of increasing concentrations of adenosine (0.1–100 μM) demonstrated its ability to biphasically modulate the evoked release of glutamate from striatal nerve terminals. At a concentration of 0.1 μM, adenosine did not significantly modify glutamate release ($n = 6$); at 1 μM, adenosine significantly decreased (23.6 ± 4.7%; $n = 8$; $p < 0.05$), whereas, at 10 and 100 μM, it significantly facilitated K^+-evoked [^{3}H]glutamate (30.4 ± 7.5 and 17.6 ± 3.5%; $n = 6$; $p < 0.05$ in both cases).

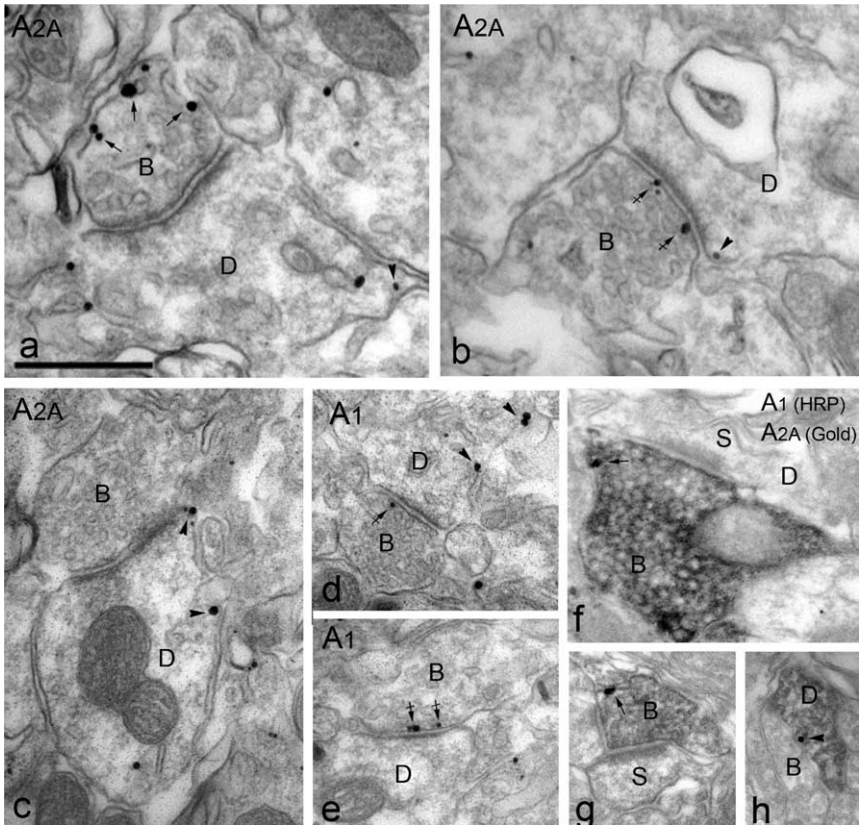

Figure 3. A_1R–A_{2A}R colocalization in rat striatum. ***a–c***, Immunogold particles for the A_{2A}Rs were observed at the presynaptic level along the extrasynaptic plasma membrane (arrows) of axon terminal (B), as well as in the presynaptic active zone (crossed arrows), facing dendritic shafts (D) and spines. A_{2A}Rs were also observed at the postsynaptic level along the extrasynaptic and perisynaptic plasma membrane of dendritic shafts (D) and spines (arrowheads), establishing asymmetrical synapses with axon terminals. ***d***, ***e***, Similarly to A_{2A}Rs, immunogold particles for the A_1R were localized along the presynaptic active zone of axon terminals (B; crossed arrows) and along the extrasynaptic plasma membrane of dendritic shafts (D) and spines (arrowheads) establishing asymmetrical synapses with axon terminals. ***f***, ***g***, Presynaptic colocalization of A_1Rs and A_{2A}Rs. Peroxidase reaction product (immunoreactivity for A_1Rs) filled axon terminals (B) establishing asymmetrical synapses with dendritic shafts (D) or spines (S), in which immunoparticles (immunoreactivity for A_{2A}Rs) were localized along the extrasynaptic plasma membrane (arrows). ***h***, Postsynaptic colocalization of A_1Rs and A_{2A}Rs. Peroxidase reaction product (immunoreactivity for A_1Rs) filled dendritic shafts (D) establishing asymmetrical synapses with axon terminals (B), in which immunoparticles (immunoreactivity for A_{2A}Rs) were localized along the synaptic plasma membrane (arrowhead). Scale bar, 0.2 μm.

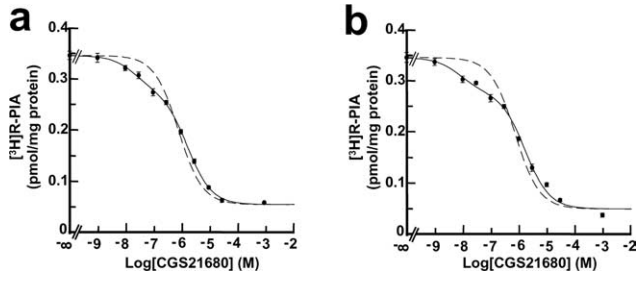

Figure 4. Intramembrane A_1R–A_{2A}R interaction in rat striatum. Effect of chronic caffeine treatment. Modulation of [^{3}H]R-PIA binding to A_1Rs by A_{2A}R activation. Striatal membranes (0.25 mg/ml) of control (***a***) or caffeine-treated rats (***b***) were incubated with 0.9 nM [^{3}H]R-PIA in the absence or presence of increasing concentrations of CGS21680 in 50 mM Tris-HCl containing 10 mM MgCl2 and 2 U/ml adenosine deaminase. Binding experiments were performed as described in Materials and Methods. The data were adjusted to one single binding site (dashed line) or to two binding sites (solid line).

A_1R–A_{2A}R intramembrane interaction and caffeine tolerance

An unresolved issue about caffeine is the strong tolerance for many of its behavioral and biochemical effects that develop after chronic treatment (Holtzman and Finn, 1988; Jacobson et al.,

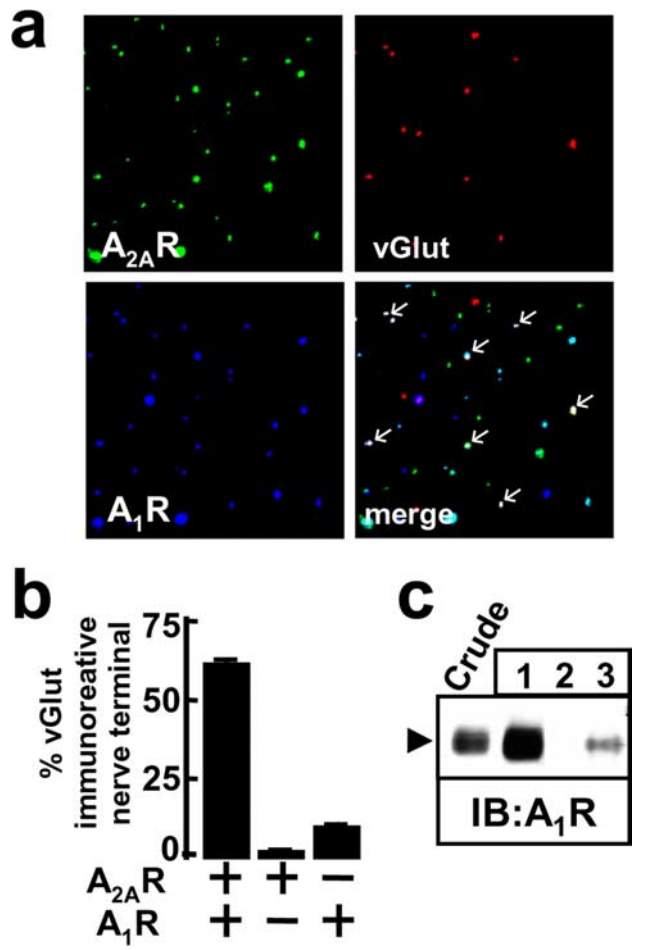

Figure 5. Adenosine receptors in glutamatergic striatal nerve terminals. ***a***, Immunocytochemical identification of $A_{2A}R$ (green) and A_1R (blue) in the glutamatergic population of rat striatal nerve terminals (identified as vGluT-1 and vGluT-2 immunoreactive; red). In the superimposed picture of this triple-immunocytochemical labeling (merge) of this representative field, the arrows indicate the $A_1R/A_{2A}R$/vGluT-containing nerve terminals. ***b***, The quantification of images of three different fields per coverslip from four experiments using different synaptosomal preparations from different animals confirmed the predominant colocalization of A_1Rs and $A_{2A}Rs$ in rat striatal glutamatergic terminals (results are means ± SEM). ***c***, Coimmunoprecipitation of A_1R and $A_{2A}R$ from rat striatal synaptosomes. Solubilized synaptosomes were immunoprecipitated using rabbit anti-A_1R polyclonal antibody (5 μg) (lane 1), irrelevant rabbit polyclonal antibody (5 μg) (lane 2), and mouse anti-$A_{2A}R$ monoclonal antibody (2 μg) (lane 3). Solubilized membranes (Crude) and immunoprecipitates (lanes 1–3) were analyzed by SDS-PAGE and immunoblotted using rabbit rabbit anti-A_1R antibody (1:1000) and HRP-conjugated swine anti-rabbit IgG as a secondary antibody. IB, Immunoblot.

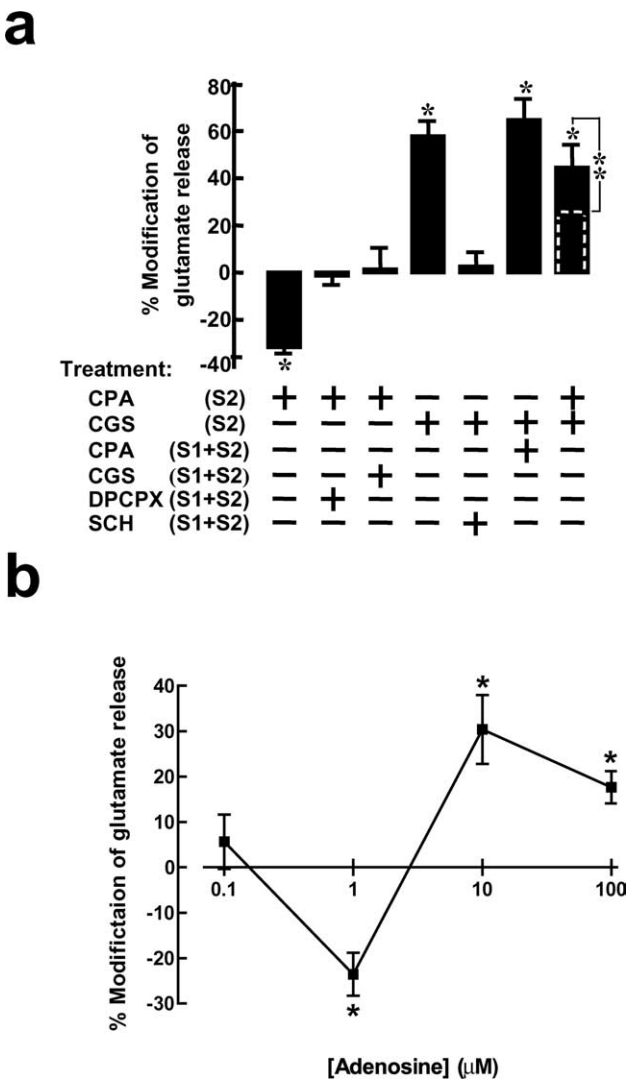

Figure 6. Effect of A_1R and $A_{2A}R$ activation on evoked release of glutamate from striatal nerve terminals. Superfused synaptosomes, previously loaded with [^{3}H]glutamate, were chemically (20 mM K^+ for 30 s) stimulated twice (S1 and S2). ***a***, CPA (100 nM) and CGS21680 (10 nM), present in S2, inhibited and facilitated, respectively, the evoked release of glutamate in a manner prevented by the A_1R and $A_{2A}R$ antagonists DPCPX (50 nM) and SCH58261 (50 nM), respectively (present in S1 and S2). The inhibitory effect of CPA (100 nM) was also abolished when CGS21680 (10 nM) was present during S1 and S2, whereas the facilitatory effect of CGS21680 was not modified when CPA (100 nM) was present in S1 and S2. Coapplication of CPA (100 nM) and CGS (10 nM) in S2 facilitated the evoked release of glutamate. The dashed bar illustrates the arithmetic sum of the effects of 10 nM CGS21680 and 100 nM CPA, if these effects were purely additive. The results are means ± SEM of three to seven experiments. *$p < 0.05$ versus 0%; **$p < 0.05$ between bars. ***b***, Increasing concentrations of adenosine (0.1–100 μM) produced a biphasic effect, with with low and high concentrations inhibiting and stimulating the evoked release of glutamate, respectively. The results are means ± SEM of six to eight experiments. *$p < 0.05$ versus 0%.

1996; Fredholm et al., 1999). To test a possible role of A_1R–$A_{2A}R$ heteromers in this phenomenon, competitive–inhibition experiments of [^{3}H]R-PIA binding using CGS21680 were performed in striatal membrane preparations of caffeine-treated rats (1 mg/ml in the drinking water for 14 d; average caffeine consumption, mean ± SEM, 120 ± 4 $mg \cdot kg^{-1} \cdot d^{-1}$), and the results compared with those obtained in naive animals. Again, the displacement curve of [^{3}H]R-PIA binding by CGS21680 in striatal membranes from caffeine-treated rats was significantly ($p < 0.001$) better fitted by a two-site model than by a single-site model (Fig. 4*b*). The IC_{50} value (mean ± SEM) corresponding to the binding of CGS21680 to A_1R (1.7 ± 0.5 mM) was similar to that obtained in naive rats (1.8 ± 0.5 μM) as well as the [^{3}H]R-PIA binding to these striatal membranes when no displacer was present (Fig. 4). However, the inhibition of the [^{3}H]R-PIA binding to A_1R when CGS21680 binds to the $A_{2A}R$ displayed an EC_{50} value about threefold lower than the value obtained in naive rats (mean ± SEM, 8 ± 3 and 22 ± 6 nM, respectively). These results indicate that caffeine pretreatment alters the function of the A_1R–$A_{2A}R$ heteromers, increasing significantly ($p < 0.02$) the potency of an A_{2A} agonist to modulate A_1Rs. The agonist binding characteristics for both striatal A_1R and $A_{2A}R$ were not modified by caffeine treatment. Thus, in competition experiments using [^{3}H]R-PIA, K_D values (means ± SEM) for the binding of R-PIA to A_1R in control and caffeine-treated animals were 0.1 ± 0.05 and 0.13 ± 0.06 nM, respectively. In competition experiments using

[^{3}H]CGS21680, K_D values for the binding of CGS21680 to $A_{2A}R$ in control and caffeine-treated animals were 111 ± 43 and 120 ± 60 nM, respectively. However, $A_{2A}Rs$ displayed a lower affinity for caffeine in membranes from caffeine-pretreated rats (K_D = 290 ± 80 μM) compared with control rats (K_D = 80 ± 10 μM). This effect was significant ($p < 0.001$) and specific for $A_{2A}Rs$, because the A_1Rs had the same affinity for caffeine in both naive and caffeine-treated animals (K_D = 19 ± 5 and 13 ± 6 μM).

Discussion

Either A_1Rs or $A_{2A}Rs$ are capable of forming heteromers with other G-protein receptors, such as dopamine, glutamate, and ATP receptors (Agnati et al., 2003). However, the existence of heteromers constituted by different adenosine receptor subtypes had not been reported. In the present study, a precise colocalization of A_1Rs and $A_{2A}Rs$ at the presynaptic level of striatal glutamatergic synapses was demonstrated by ultrastructural analysis. The results of immunocytochemistry and coimmunoprecipitation experiments showed that the striatal A_1R–$A_{2A}R$ heteromer is preferentially localized in the striatal glutamatergic terminals, and the experiments of evoked glutamate release directly demonstrated the ability of presynaptic $A_{2A}Rs$ to control the A_1R-mediated modulation of striatal glutamate release. Radioligand-binding experiments demonstrated that a main biochemical characteristic of the A_1R–$A_{2A}R$ heteromer is the ability of $A_{2A}R$ activation to reduce the affinity of the A_1R for agonists. Together, the present results indicate that the A_1R–$A_{2A}R$ heteromer plays a role in the adenosine-mediated fine-tuning modulation of striatal glutamatergic neurotransmission.

Under basal conditions, the relatively low extracellular levels of adenosine preferentially stimulate A_1Rs, which show a higher affinity for adenosine than $A_{2A}Rs$ (Fredholm et al., 2001). The preferential A_1R stimulation in the A_1R–$A_{2A}R$ heteromer inhibits glutamatergic neurotransmission. Under conditions of stronger adenosine release, A_{2A} receptor activation in the A_1R–$A_{2A}R$ heteromer would block A_1R-mediated function, and the overall result will be a facilitation of the evoked release of glutamate (supplemental figure, available at www.jneurosci.org as supplemental material). Thus, the functional characteristics of the A_1R–$A_{2A}R$ heteromers are different from A_1 or A_{2A} receptors and provide a rationale to understand how adenosine might facilitate or inhibit glutamatergic transmission depending on the concentration of adenosine. In fact, increasing concentrations of adenosine demonstrated a biphasic effect, with low and high concentrations of adenosine inhibiting and stimulating glutamate release from striatal nerve terminals, respectively.

The present study also provides new information about the main pharmacological targets of caffeine, A_1Rs and $A_{2A}Rs$. To our knowledge, this is the first study that analyses simultaneously the affinity of A_1Rs and $A_{2A}Rs$ for caffeine in transfected cells and brain (striatal) tissue. Previous studies using cloned transfected receptors showed that $A_{2A}R$ displays higher affinity for caffeine than A_1R (Fredholm et al., 1999, 2001). In contrast, the results obtained from brain tissue are more variable, showing either no difference (Muller et al., 1997), a preferential affinity of $A_{2A}R$ (Svenningsson et al., 1999), or a preferential affinity of A_1R for caffeine (Antoniou et al., 2005). Significant differences in the affinity of $A_{2A}R$ for caffeine were observed depending on its selective association with A_1R. In agreement with previous studies (Fredholm et al., 2001), $A_{2A}Rs$ display higher affinity for caffeine than A_1Rs when studied in single-transfected cells. However, A_1R–$A_{2A}R$, but not $A_{2A}R$–D_2R, heteromerization was associated with a prominent decrease in the affinity of $A_{2A}R$ for caffeine, with a K_D value comparable with that observed in striatal tissue. Taking also into account that the "biochemical fingerprint" of the A_1R–$A_{2A}R$ heteromer (the ability of $A_{2A}R$ activation to reduce the affinity of the A_1R for agonists) could be demonstrated in striatal membrane preparations, the present results indicate that a significant amount of striatal A_{2A} receptors are forming heteromers with A_1Rs. However, although most A_1Rs and $A_{2A}Rs$ localized in the glutamatergic terminals are forming part of A_1R–$A_{2A}R$ heteromers, in the striatum caffeine can also target $A_{2A}Rs$ not interacting with A_1Rs localized in the dendritic spine of GABAergic enkephalinergic neurons (Rosin et al., 2003), where they can form heteromers with dopamine D_2R or metabotropic $mGlu_5$ receptors (Ferré et al., 2002; Agnati et al., 2003; Canals et al., 2003). In fact, $A_{2A}R$ in the A_{2A}-D_2R heteromer has a higher affinity for caffeine than the $A_{2A}R$ in the A_1R–$A_{2A}R$ heteromer (Table 1). The blockade of these postsynaptic $A_{2A}Rs$ could explain the decrease in the striatal expression of immediate-early genes and preproenkephalin mRNA and increased phosphorylation of DARPP-32 (dopamine- and cAMP-regulated phosphoprotein 32) (at threonine 75) described after acute caffeine treatments (Svenningsson et al., 1995; Lindskog et al., 2002).

The functional characteristics of the A_1R–$A_{2A}R$ heteromers also allow understanding the different effects operated under acute and chronic caffeine administration. Because at relatively low adenosine levels there is little occupancy of $A_{2A}Rs$, most of the behavioral and biochemical effects after an acute administration of caffeine are most probably attributable to A_1R blockade (Snyder et al., 1981; Solinas et al., 2002, 2005; Karcz-Kubicha et al., 2003; Quarta et al., 2004a,b; Antoniou et al., 2005). In fact, the acute systemic or intrastriatal administration of caffeine enhances striatal glutamate release (Solinas et al., 2002; Quarta et al., 2004a,b). A significant finding of the present study was the increased antagonistic interaction between A_1R and $A_{2A}R$ in the A_1R–$A_{2A}R$ heteromer with chronic caffeine treatment. But, apart from the affinity of the A_1R and $A_{2A}R$ for adenosine and caffeine and the A_1R–$A_{2A}R$ intramembrane interaction, one more variable plays a substantial role when analyzing the effects taking place after chronic caffeine administration. Chronic treatment with the methylxanthine leads to an increase in the plasma and extracellular levels of adenosine (Conlay et al., 1997; Andresen et al., 1999). The same treatment with caffeine (1 mg/ml in the drinking water for 14 d) used in the present study was reported to produce a 10-fold increase in plasma adenosine levels (Conlay et al., 1997). Under chronic caffeine treatment (or other conditions leading to increased adenosine levels), adenosine also binds and activates $A_{2A}R$, which, in addition, has a reduced affinity for caffeine. This likely scenario would lead to a situation in which the increased levels of adenosine acting on $A_{2A}R$ would potently inhibit A_1R function by means of the increased A_1R–$A_{2A}R$ intramembrane interaction. Under these conditions, caffeine would have little effect on A_1Rs, which would already be inhibited as a consequence of the increased A_1R–$A_{2A}R$ intramembrane intermolecular interaction. In fact, recent studies show a predominant $A_{2A}R$ antagonist behavioral and biochemical profile of caffeine under chronic administration with tolerance to its A_1R antagonistic effects (Karcz-Kubicha et al., 2003; Quarta et al., 2004a). The present results suggest that an increased A_1R–$A_{2A}R$ interaction in the A_1R–$A_{2A}R$ heteromer is involved in the tolerance to the psychostimulant effects of caffeine.

In conclusion, we have demonstrated that A_1Rs and $A_{2A}Rs$ can form heteromers in striatum where they modulate glutamatergic neurotransmission and whose existence may help in comprehending the mechanisms underlying the behavioral effects pro-

duced by acute or chronic consumption of caffeine, the most consumed psychoactive drug in the world.

References

Agnati LF, Ferré S, Lluis C, Franco R, Fuxe K (2003) Molecular mechanisms and therapeutical implications of intramembrane receptor/receptor interactions among heptahelical receptors with examples from the striatopallidal GABA neurons. Pharmacol Rev 55:509–550.

Andresen BT, Gillespie DG, Mi Z, Dubey RK, Jackson EK (1999) Role of adenosine A(1) receptors in modulating extracellular adenosine levels. J Pharmacol Exp Ther 291:76–80.

Antoniou K, Papadopoulou-Daifoti Z, Hyphantis T, Papathanasiou G, Bekris E, Marselos M, Muller M, Goldberg SR, Ferré S (2005) A detailed behavioral analysis on the motor effects of caffeine and the involvement of adenosine A1 and A2A receptors in the rat. Psychopharmacology 183:154–162.

Canals M, Marcellino D, Fanelli F, Ciruela F, de Benedetti P, Goldberg SR, Neve K, Fuxe K, Agnati LF, Woods AS, Ferré S, Lluis C, Bouvier M, Franco R (2003) Adenosine A2A-dopamine D2 receptor-receptor heteromerization: qualitative and quantitative assessment by fluorescence and bioluminescence energy transfer. J Biol Chem 278:46741–46749.

Casadó V, Canti C, Mallol J, Canela EI, Lluis C, Franco R (1990) Solubilization of A1 adenosine receptor from pig brain: characterization and evidence of the role of the cell membrane on the coexistence of high- and low-affinity states. J Neurosci Res 26:461–473.

Casadó V, Casillas T, Mallol J, Canela EI, Lluis C, Franco R (1992) The adenosine receptors present on the plasma membrane of chromaffin cells are of the A2b subtype. J Neurochem 59:425–431.

Cheng YC, Prusoff WH (1973) Relationship between the inhibition constant (K1) and the concentration of inhibitor which causes 50 percent inhibition (I50) of an enzymatic reaction. Biochem Pharmacol 22:3099–3108.

Ciruela F, Escriche M, Burgueno J, Angulo E, Casado V, Soloviev MM, Canela EI, Mallol J, Chan WY, Lluis C, McIlhinney RA, Franco R (2001) Metabotropic glutamate 1alpha and adenosine A1 receptors assemble into functionally interacting complexes. J Biol Chem 276:18345–18351.

Conlay LA, Conant JA, deBros F, Wurtman R (1997) Caffeine alters plasma adenosine levels. Nature 389:136.

Dunwiddie TV, Masino SA (2001) The role and regulation of adenosine in the central nervous system. Annu Rev Neurosci 24:31–55.

Ferré S, Karcz-Kubicha M, Hope BT, Popoli P, Burgueno J, Gutierrez MA, Casado V, Fuxe K, Goldberg SR, Lluis C, Franco R, Ciruela F (2002) Synergistic interaction between adenosine A2A and glutamate mGlu5 receptors: implications for striatal neuronal function. Proc Natl Acad Sci USA 99:11940–11945.

Fredholm BB, Battig K, Holmen J, Nehlig A, Zvartau EE (1999) Actions of caffeine in the brain with special reference to factors that contribute to its widespread use. Pharmacol Rev 51:83–133.

Fredholm BB, Irenius E, Kull B, Schulte G (2001) Comparison of the potency of adenosine as an agonist at human adenosine receptors expressed in Chinese hamster ovary cells. Biochem Pharmacol 61:443–448.

Fremeau Jr RT, Troyer MD, Pahner I, Nygaard GO, Tran CH, Reimer RJ, Bellocchio EE, Fortin D, Storm-Mathisen J, Edwards RH (2001) The expression of vesicular glutamate transporters defines two classes of excitatory synapse. Neuron 31:247–260.

Herrera C, Casadó V, Ciruela F, Schofield P, Mallol J, Lluis C, Franco R (2001) Adenosine A2B receptors behave as an alternative anchoring protein for cell surface adenosine deaminase in lymphocytes and cultured cells. Mol Pharmacol 59:127–134.

Herzog E, Bellenchi GC, Gras C, Bernard V, Ravassard P, Bedet C, Gasnier B, Giros B, El Mestikawy S (2001) The existence of a second vesicular glutamate transporter specifies subpopulations of glutamatergic neurons. J Neurosci 21:RC181(1–6).

Holtzman SG, Finn IB (1988) Tolerance to behavioral effects of caffeine in rats. Pharmacol Biochem Behav 29:411–418.

Jacobson KA, von Lubitz DK, Daly JW, Fredholm BB (1996) Adenosine receptor ligands: differences with acute versus chronic treatment. Trends Pharmacol Sci 17:108–113.

Karcz-Kubicha M, Antoniou K, Terasmaa A, Quarta D, Solinas M, Justinova A, Pezzola R, Reggio CE, Müller K, Fuxe SR, Goldberg P, Popoli P, Ferré S (2003) Involvement of adenosine A_1 and A_{2A} receptors in the motor effects of caffeine after its acute and chronic administration. Neuropsychopharmacology 28:1281–1291.

Lindskog M, Svenningsson P, Pozzi L, Kim Y, Fienberg AA, Bibb JA, Fredholm BB, Nairn AC, Greengard P, Fisone G (2002) Involvement of DARPP-32 phosphorylation in the stimulant action of caffeine. Nature 418:774–778.

Lopes LV, Cunha RA, Kull B, Fredholm BB, Ribeiro JA (2002) Adenosine A(2A) receptor facilitation of hippocampal synaptic transmission is dependent on tonic A(1) receptor inhibition. Neuroscience 112:319–329.

Lujan R, Nusser Z, Roberts JD, Shigemoto R, Somogyi P (1996) Perisynaptic location of metabotropic glutamate receptors mGluR1 and mGluR5 on dendrites and dendritic spines in the rat hippocampus. Eur J Neurosci 8:1488–1500.

McVey M, Ramsay D, Kellett E, Rees S, Wilson S, Pope AJ, Milligan G (2001) Monitoring receptor oligomerization using time-resolved fluorescence resonance energy transfer and bioluminescence resonance energy transfer. The human delta-opioid receptor displays constitutive oligomerization at the cell surface, which is not regulated by receptor occupancy. J Biol Chem 276:14092–14099.

Muller CE, Geis U, Hipp J, Schobert U, Frobenius W, Pawlowski M, Suzuki F, Sandoval-Ramirez J (1997) Synthesis and structure-activity relationships of 3,7-dimethyl-1-propargylxanthine derivatives, A2A-selective adenosine receptor antagonists. J Med Chem 40:4396–4405.

O'Kane EM, Stone TW (1998) Interaction between adenosine A1 and A2 receptor-mediated responses in the rat hippocampus in vitro. Eur J Pharmacol 362:17–25.

Quarta D, Ferré S, Solinas M, You Z-B, Hockemeyer J, Popoli P, Goldberg SR (2004a) Opposite modulatory roles for adenosine A1 and A2A receptors on glutamate and dopamine release in the shell of the nucleus accumbens. Effects of chronic caffeine exposure. J Neurochem 88:1151–1158.

Quarta D, Borycz J, Solinas M, Patkar K, Hockemeyer J, Ciruela F, Lluis C, Franco R, Woods AS, Goldberg SR, Ferré S (2004b) Adenosine receptor-mediated modulation of dopamine release in the nucleus accumbens depends on glutamate neurotransmission and *N*-methyl-D-aspartate receptor stimulation. J Neurochem 91:873–880.

Rodrigues RJ, Alfaro TM, Rebola N, Oliveira CR, Cunha RA (2005) Co-localization and functional interaction between adenosine A(2A) and metabotropic group 5 receptors in glutamatergic nerve terminals of the rat striatum. J Neurochem 92:433–441.

Rosin DL, Hettinger BD, Lee A, Linden J (2003) Anatomy of adenosine A2A receptors in brain: morphological substrates for integration of striatal function. Neurology 61:S12–S18.

Sarrió S, Casadó V, Escriche M, Ciruela F, Mallol J, Canela EI, Lluis C, Franco R (2000) The heat shock cognate protein hsc73 assembles with A(1) adenosine receptors to form functional modules in the cell membrane. Mol Cell Biol 20:5164–5174.

Snyder SH, Katims JJ, Annau Z, Bruns RF, Daly JW (1981) Adenosine receptors and behavioral actions of methylxanthines. Proc Natl Acad Sci USA 78:3260–3264.

Solinas M, Ferré S, You Z-B, Karcz-Kubicha M, Popoli P, Goldberg SR (2002) Caffeine induces dopamine and glutamate release in the shell of the nucleus accumbens. J Neurosci 22:6321–6324.

Solinas S, Ferré S, Antoniou K, Quarta D, Justinova Z, Hockemeyer J, Pappas LA, Segal P, Wertheim C, Müller CE, Goldberg SR (2005) Involvement of adenosine A1 receptors in the discriminative-stimulus effects of caffeine. Psychopharmacology 179:576–586.

Svenningsson P, Nomikos GG, Fredholm BB (1995) Biphasic changes in locomotor behavior and in expression of mRNA for NGFI-A and NGFI-B in rat striatum following acute caffeine administration. J Neurosci 15:7612–7624.

Svenningsson P, Nomikos GG, Fredholm BB (1999) The stimulatory action and the development of tolerance to caffeine is associated with alterations in gene expression in specific brain regions J Neurosci 19:4011–4022.

Wu LG, Saggau P (1997) Presynaptic inhibition of elicited neurotransmitter release. Trends Neurosci 20:204–212.

Yawo H, Chuhma N (1993) Preferential inhibition of omega-conotoxin-sensitive presynaptic Ca^{2+} channels by adenosine autoreceptors. Nature 365:256–258.